ELSEVIER

Journal of Power Sources 73 (1998) 216–223

JOURNAL OF POWER SOURCES

Electrochemical characterization of tin based composite oxides as negative electrodes for lithium batteries

Stefan Machill, Takahisa Shodai *, Yoji Sakurai, Jun-ichi Yamaki [1]

NTT Integrated Information and Energy Systems Laboratories, Tokai-mura, Naka-gun, Ibaraki-ken 319-11, Japan

Received 10 June 1997; accepted 5 December 1997

Abstract

Amorphous tin containing composite oxides are a promising negative electrode material for rechargeable lithium batteries. We have investigated the electrochemical behaviour of several $SnB_xP_yO_z$ compounds vs. metallic lithium in cells containing 1 M $LiClO_4$ dissolved in ethylenecarbonate/1,2-diethoxyethane as the electrolyte. We have determined the relationship between the composition of the active electrode material and the cycling performance. Furthermore, we examined the influence of structural changes caused by single roll quenching. We also investigated the influence of the choice of phosphorus supplying starting material.

Keywords: Amorphous tin composite oxides; Lithium battery; Anode

1. Introduction

In recent years there has been a growing interest in the development of new negative electrode materials for rechargeable lithium batteries [1]. This trend was caused by the introduction of the lithium-ion concept. Carbonaceous materials were developed as high capacity negative electrodes (theoretical capacity of 372 mAh/g based on LiC_6). Now, these materials are accepted and used in nearly all lithium-ion batteries.

In addition, various oxide and nitride materials have been investigated for application to lithium-ion batteries. Compounds derived from Li_3N lithium transition metal nitrides such as $Li_{2.6}Co_{0.4}N$ have been developed which perform well as anode materials [2]. Oxides such as $Li_{4/3}Ti_{5/3}O_4$ [3], MoO_2, WO_2 and Fe_2O_3 offer a slightly lower capacity at a higher potential. Because of their potential some of these materials were first examined as positive electrodes in combination with metallic lithium. The development of high potential (4V) cathodes has led to a greater interest in these materials as negative electrodes [4].

Stimulated by work undertaken by Fuji Photo Film, research activity is now focused on amorphous tin-based composite oxides [5–9]. According to Idota et al. [5] these materials provide a very high reversible gravimetric capacity of >600 mAh/g. This is about twice the theoretical capacity of carbon. Basically, the composite oxides consist of SnO units in a network of glass forming elements such as boron or phosphorus. SnO itself is one of the compounds originally investigated as cathode material [10]. Their low cell voltage meant that Li/SnO cells could not achieve any practical importance. However, when embedded in a glass network these oxides behave very differently.

Here, we report on the electrochemical properties of several $SnO–B_2O_3–P_2O_5$ composite oxides.

2. Experimental

2.1. Material preparation

We synthesized several $SnB_xP_yO_z$ compounds by mixing reagent grade SnO (Showa Chemicals), B_2O_3 and P_2O_5 (both Kanto Chemical) in appropriate amounts as shown in Table 1. The compound $SnB_{0.5}P_{0.5}O_3$ was also prepared from $SnHPO_4$ (Sn dissolved in H_3PO_4) or $Sn_2P_2O_7$ (Aldrich) as the phosphorus supplying component. The mixtures were melted for 4 h at 1000°C in a sintered alumina crucible in an argon atmosphere. The

* Corresponding author.

[1] Present address: Institute of Advanced Material Study, Department of Molecular Science and Technology, Kyushu University, 6-1, Kasuga-koen, Kasuga-shi, Fukuoka 816, Japan.

0378-7753/98/$19.00

Table 1
Molar composition of the several invastigated oxides

SnO	B_2O_3	P_2O_5	Composite oxide
1	0.25	0.25	$SnB_{0.5}P_{0.5}O_3$
1	0.3	0.2	$SnB_{0.6}P_{0.4}O_{2.9}$
1	0.2	0.3	$SnB_{0.4}P_{0.6}O_{3.1}$
2	0.25	0.25 $Sn_2P_2O_7$	$Sn2B_{0.5}P_{0.5}O_4$
0.5	0.25	0.25 $SnHPO_4$	$SnB_{0.5}P_{0.5}O_3$
0.5	0.25	0.5	$SnB_{0.5}P_{0.5}O_3$

heating and cooling rates were both about 200°C/h. By melting the starting materials in an $Ar:O_2$ (1:1) atmosphere we obtained the oxygen rich material $SnB_{0.5}P_{0.5}O_{3+x}$. This material was a compact yellow glass, whose colour had a varied in intensity depending on the composition. The so-called fast-quenched $SnB_{0.5}P_{0.5}O_3$ was treated by the single-roll quenching technique.

2.2. Cell assembly

After preparation the samples were ground in an agate mortar and mixed with 25 wt.% acetylene black (Denki

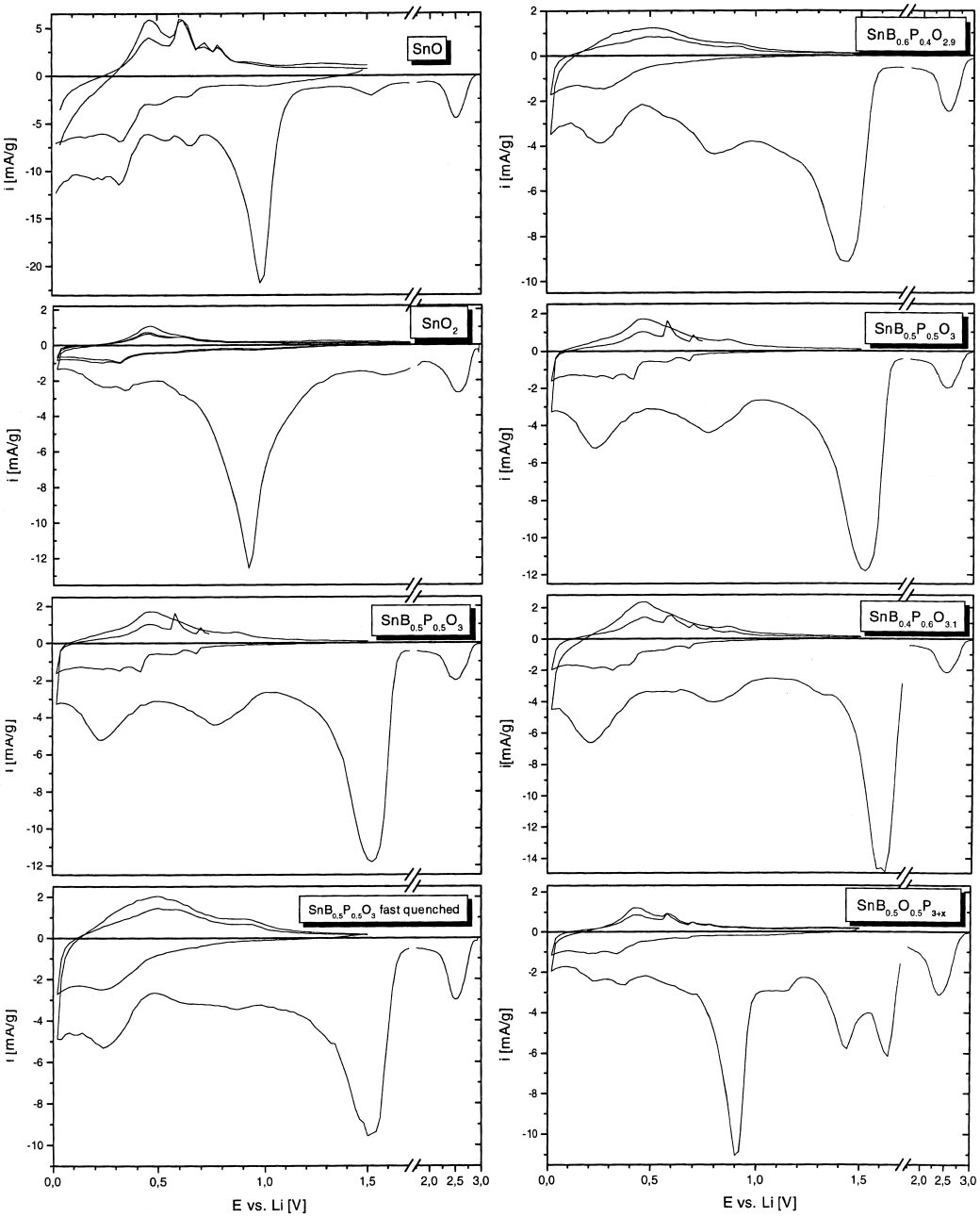

Fig. 1. Cyclic voltammograms of SnO, SnO_2 and several $SnO–B_2O_3–P_2O_5$ composite oxides; sweep rate: stepwise 20 mV every 2 h starting from 3.0 V.

Kagaku) and 5 wt.% polytetrafluoroethylene powder (Daikin) as binder. The mixture was then pressed and cut into pellets (15 mm in diameter, and about 0.3 mm thick).

For our electrochemical investigations we fabricated coin-type cells (type R2320) with the sample electrode and a Li metal (Honjo Metal) counter electrode. A microporous polypropylene film (Celgard 3501, Hoechst Celanese) was used as a separator. The electrolyte we used was 1 M $LiClO_4$ dissolved in ethylenecarbonate/1,2-diethoxyethane (Lipaste® EDEE/1 Tomiyama Pure Chemicals). All operations were carried out in a dry atmosphere.

2.3. Measuring equipment

The charge/discharge behaviour of the cells was measured galvanostatically ($I = 1$ mA) in the 0.0 V to 1.5 V range. The slow scan voltammograms were recorded with a MacPile multichannel potentiostat/galvanostat. This instrument allows to sweep the potential step by step (here 20 mV every 2 h) and records the charge increment vs. time for every step as coulometer.

The structures were characterized by X-ray powder diffraction (XRD) (Rigaku RU-200) measurements using Cu Kα radiation.

3. Results and discussion

We used slow scan dynamic voltammetry to determine the electrochemical behaviour of a tin-based composite oxide during reduction and oxidation. Starting from the open cell voltage the cells were discharged down to 0.0 V and after that cycled between 0.0 and 1.5 V. The potentials were swept stepwise by 20 mV every two hours. For every step the current i was calculated from the recorded charge increment. The results for the several materials are shown in Fig. 1.

Generally we can observe that the appearance of the first sweep from 3.0 to 0.0 V is very different from the subsequent cycles. It seems that during the first sweep certain irreversible processes occur. Regardless of which sample is used, a reduction peak can be observed at 2.6 V. This suggests that this peak must be related to a reduction reaction at another part of the composite electrode.

A large dominating reduction peak can be observed around 950 mV for SnO and SnO_2. This peak appears only during the first reduction and marks an irreversible process. According to Courtney and Dahn [7,8] these peaks must be assigned to the reduction of SnO or SnO_2 to metallic tin after the incorporation of lithium as follows [9].

$$SnO_2 + 2Li \rightarrow SnO + Li_2O \qquad E_{vs.Li} = 1.88\,V \qquad (1)$$

$$SnO + 2Li \rightarrow Sn + Li_2O \qquad E_{vs.Li} = 1.58\,V \qquad (2)$$

Moreover, further peaks appear in the reduction as well as in the oxidation sweep. These peaks are very reproducible. As suggested by several authors [7–9] these peaks may represent the different states of the storage of lithium in the form of Li_xSn_y-alloys. With SnO we can distinguish at least 4 stages of alloying. The observed current density in the SnO_2 voltammogram is lower than that with SnO.

The situation is very different with the tin based composite oxides we investigated. For all the investigated materials except for the oxygen rich $SnB_{0.5}P_{0.5}O_{3+x}$ the dominating irreversible reduction peak appears around 1.5 V. This is nearer to the expected theoretical values reported by Huggins [9] for the reduction processes in Eqs. (1) and (2). Furthermore, two clear peaks appear around

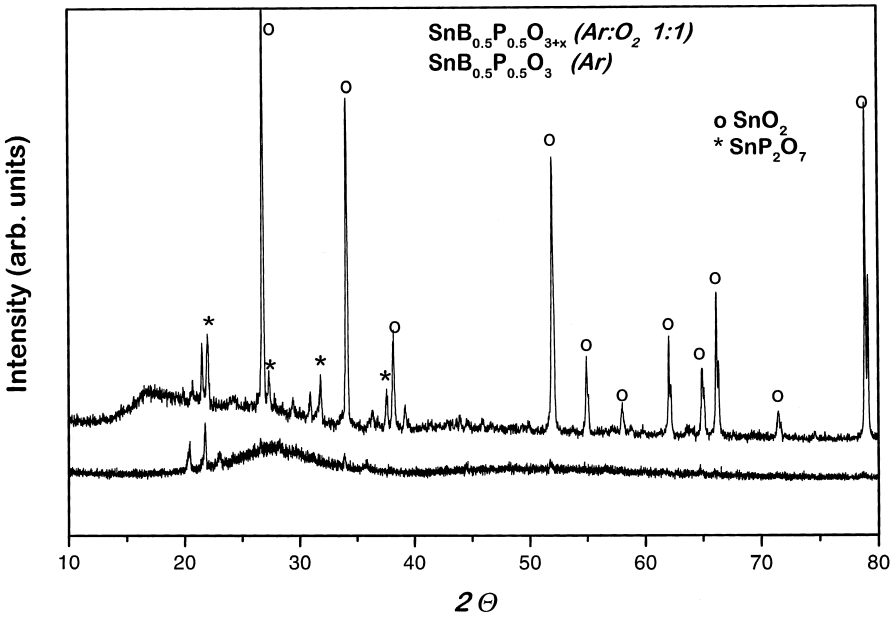

Fig. 2. X-ray diffraction patterns of $SnB_{0.5}P_{0.5}O_3$ synthesized in Ar or Ar:O_2 atmosphere.

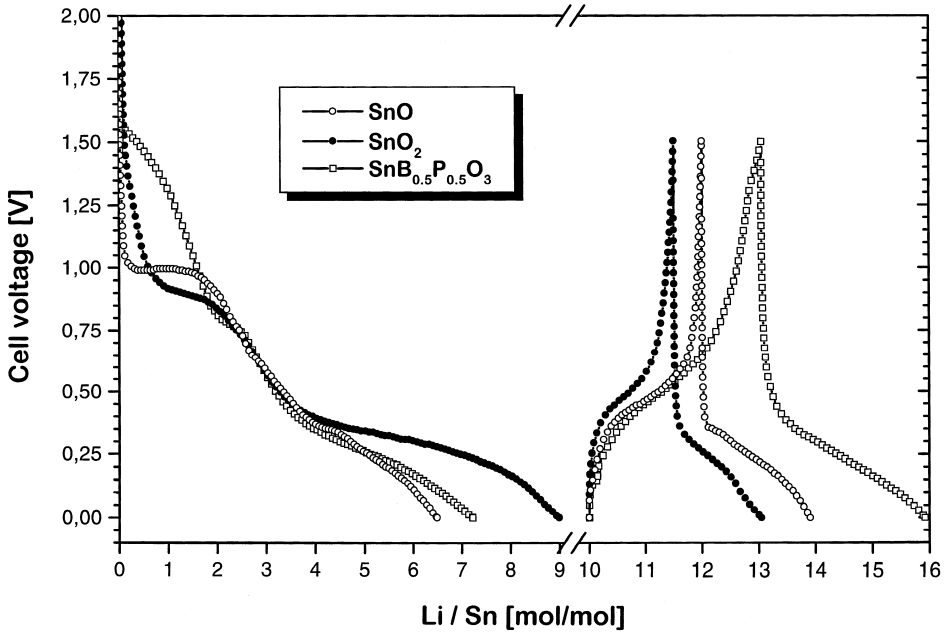

Fig. 3. Electrochemical charge–discharge characteristics of SnO, SnO_2 and $SnB_{0.5}P_{0.5}O_3$ composite oxide; $|i| = 0{,}5$ mA/cm^2.

800 mV and 250 mV. The corresponding oxidation peaks can be seen at slightly higher potentials. However, the processes which occur in the first reduction step are not completely reversible. The subsequent 1.5 steps show relatively good reversibility.

The behaviour of the voltammogram of the oxygen rich material $SnB_{0.5}P_{0.5}O_{3+x}$ was very different from that of the materials synthesized in an argon atmosphere. After starting the reduction sweep two peaks appear at 1.65 and 1.4 V. From that point on the behaviour is similar to that of pure SnO_2. That accords well with the X-ray diffraction patterns shown in Fig. 2. $SnB_{0.5}P_{0.5}O_3$ formed in an argon atmosphere shows a mainly amorphous state. By contrast, the synthesis of $SnB_{0.5}P_{0.5}O_{3+x}$ in a mixed argon–oxygen atmosphere leads to a crystallized material. All the lines for SnO_2 (cassiterite) and in addition those of tin(IV)pyrophosphate appear in the X-ray diffraction pattern of this material.

The fast quenching treatment, which results in a completely amorphous material, leads to a decrease in the current density of the peak at 800 mV.

The dependence of the voltage on the amount of reacted lithium is given in Fig. 3 for SnO, SnO_2 and $SnB_{0.5}P_{0.5}O_3$. Two plateaus were recorded in the first reduction step. For SnO and SnO_2 the first plateau appears at 1.0 V. The second one appears around 300 mV. For the composite oxide the voltage–time curve slopes down more continuously. In this curve the first plateau appears after the reduction of 2 mol lithium around 800 mV. The shapes of the voltage profiles after the initial discharge are very similar. Table 2 gives the experimentally observed amounts of lithium during the initial cycle.

Each of the reactions described in Eqs. (1) and (2) consumes a maximum of 2 mol lithium per tin. The assumption that all the lithium is stored via the formation of tin–lithium alloys (up to $Li_{4.4}Sn$) can explain the situation only in the case of SnO. For the other materials we found a greater reduction capacity. This means that there is a side reaction and/or reaction based on another mechanism. If we assume that the alloying of tin with lithium is possible up to $Li_{4.4}Sn$, the poor reversibility indicates the high probability of another reaction. With

Table 2
In Fig. 3 experimental estimated amount of Li, reduced and oxidized on several tin containing substrates during the initial cycle

Substrate	First reduction			First oxidation
	Total reduced	Formation of Sn according to Eqs. (1) and (2)	Difference	
SnO_2	9.0 mol Li	−4 mol Li	5	1.4 mol Li
SnO	6.4 mol Li	−2 mol Li	4.4	2.0 mol Li
$SnB_{0.5}P_{0.5}O_3$	7.2 mol Li	−2 mol Li	5.2	3.0 mol Li

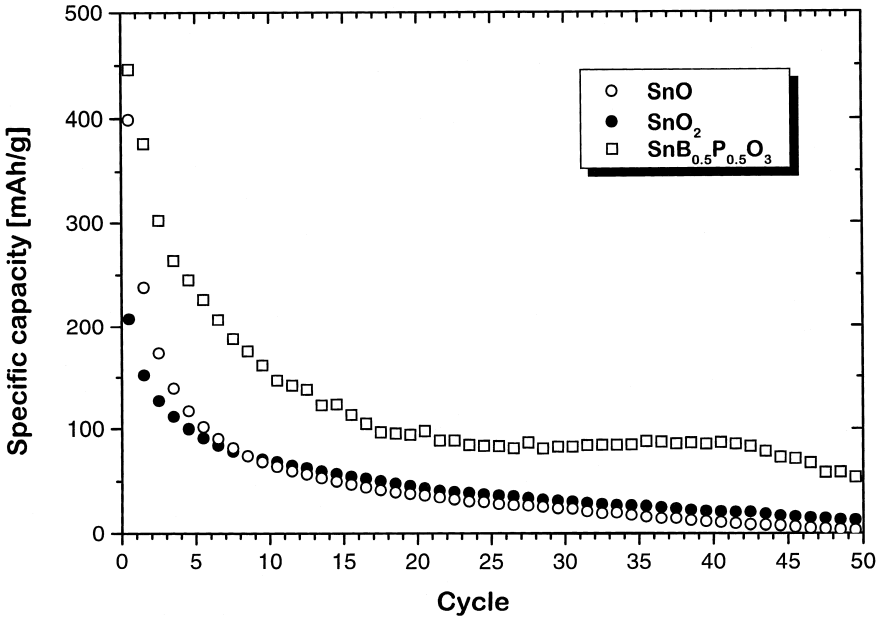

Fig. 4. Cycling performance of SnO, SnO_2 and $SnB_{0.5}P_{0.5}O_3$ composite oxide; $|i| = 0{,}5$ mA/cm^2; 0.0 V ↔ 1.5 V.

$SnB_{0.5}P_{0.5}O_3$, we found that the formation of Li_2O inside the material also influences the B_2O_3–P_2O_5 network [11].

The performance of the materials was estimated by galvanostatic cycling between 0.0 and 1.5 V with a current density of 0.5 mA/cm^2. The discharge capacities for the initial 50 cycles are shown in Fig. 4. The capacities of all three materials decrease dramatically over the first 10 cycles. After that, in the case of $SnB_{0.5}P_{0.5}O_3$, the capacity stabilizes around 100 mAh/g. For SnO and SnO_2, the capacity falls continuously to nearly zero.

Fig. 5 shows the charge/discharge behaviour of several tin containing composite oxides during the first 1.5 cycles. The graphs are almost the same as those for $SnB_{0.5}P_{0.5}O_3$ and their appearance does not depend on the composition. Moreover, single-roll fast quenching has no influence on the charge/discharge behaviour, either. The capacities of

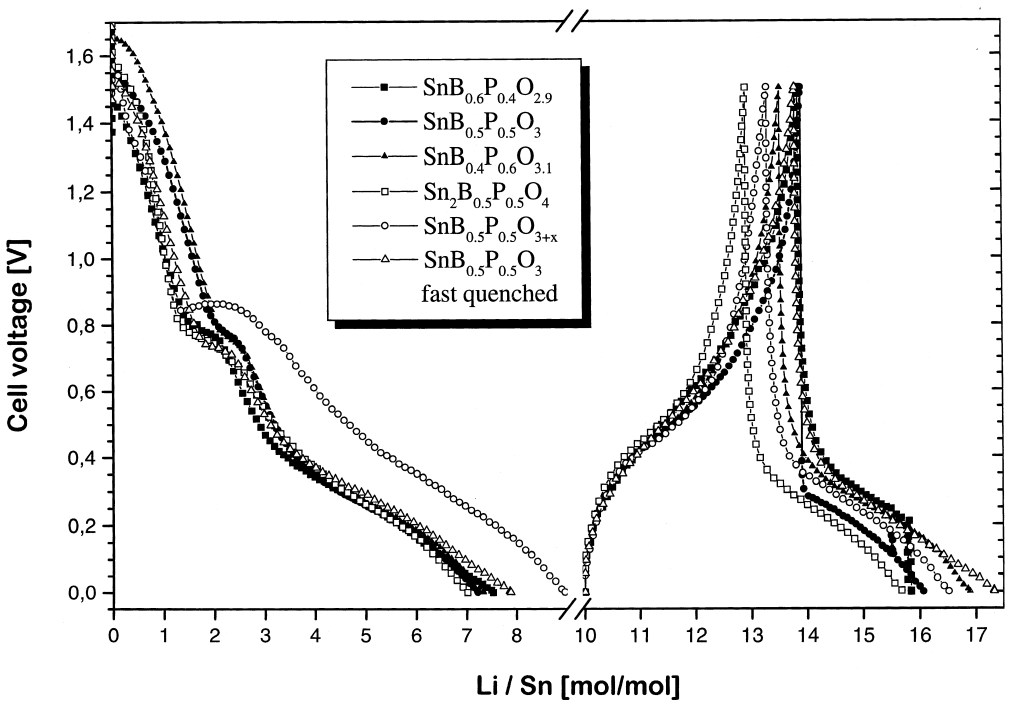

Fig. 5. Voltage–time behaviour of several SnO–B_2O_3–P_2O_5 composite oxides; $|i| = 0{,}5$ mA/cm^2.

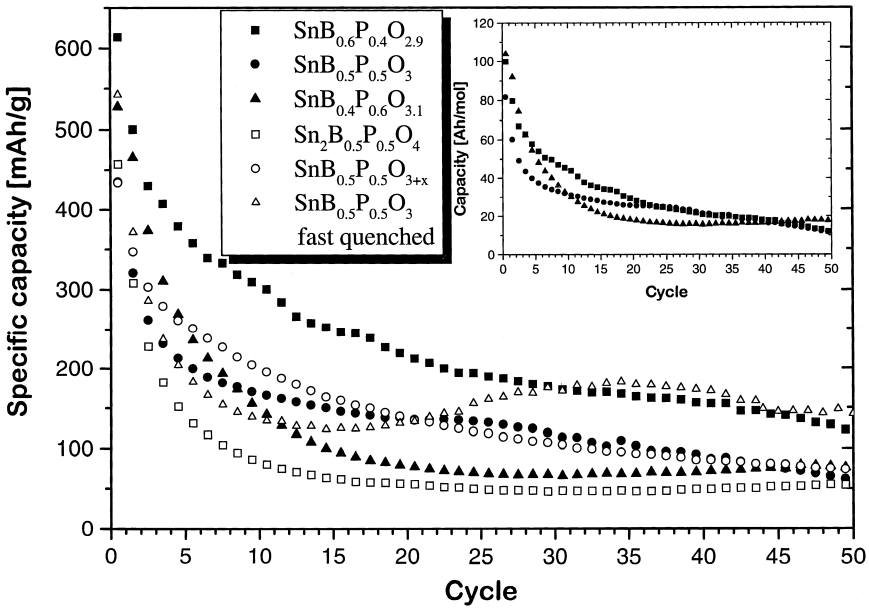

Fig. 6. Cycling performance of several $SnO–B_2O_3–P_2O_5$ composite oxides; $|i| = 0{,}5$ mA/cm^2; 0.0 V ↔ 1.5 V.

the first reduction step are around 7 Li/mol for tin composite oxide (1050 mAh/g). Only the oxygen rich $SnB_{0.5}P_{0.5}O_{3+x}$ shows exceptional behaviour. The large amount of 9 Li/mol (1150 mAh/g) can be reacted with this compound. As discussed above, here we can confirm that this material behaves in the same way as pure SnO_2, since it contains a lot of crystalline SnO_2 domains in the matrix as evidenced by XRD.

The cycling performance of several tin containing composite oxides for the first 50 cycles is given in Fig. 6. As shown in Fig. 4 the capacities generally decrease enormously, especially up to the tenth cycle. The cyclability depends only slightly on the composition. The best cyclability was observed for the composite oxide with the highest share of B_2O_3. As the P_2O_5 share increases the cycling performance decreases. If we look at the capacity related to the mol tin in the composite oxide (inset in Fig. 6) we can observe almost the same cycling behaviour for all the substrates. This means the use of a light network former component such as boron gives a higher specific

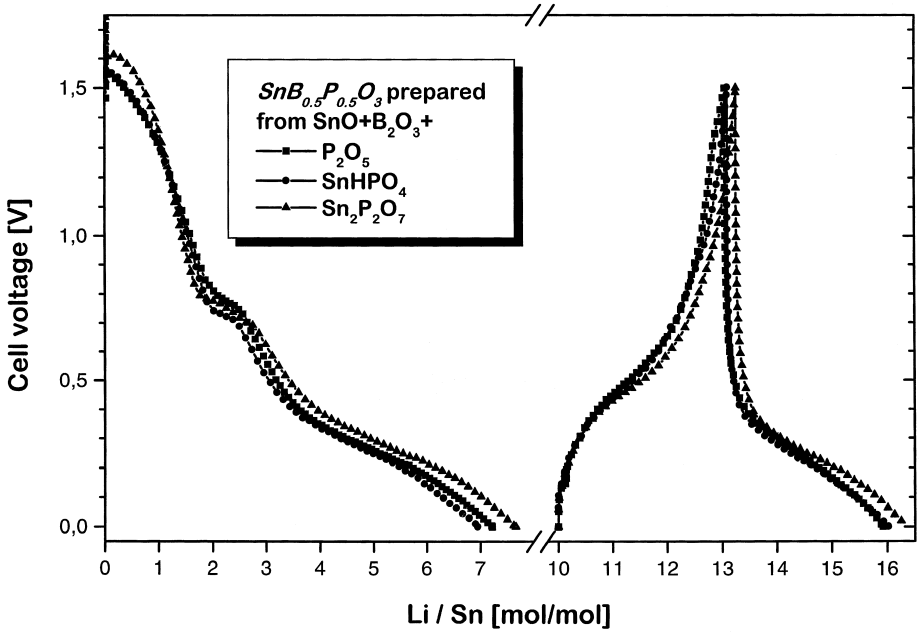

Fig. 7. Voltage–time behavior of $SnB_{0.5}P_{0.5}O_3$ composite oxides prepared from different phosphorus supplying materials; $|i| = 0{,}5$ mA/cm^2.

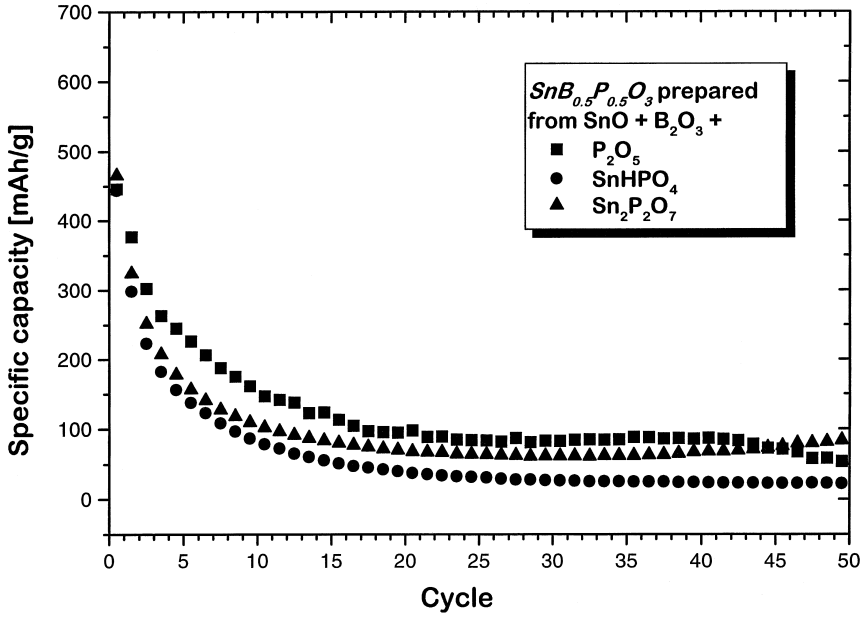

Fig. 8. Cycling performance of $SnB_{0.5}P_{0.5}O_3$ composite oxides prepared from different phosphorus supplying materials; $|i| = 0{,}5$ mA/cm^2; 0.0 V ↔ 1.5 V.

capacity. By contrast we tried to double the share of active SnO in the composite oxide ($Sn_2B_{0.5}P_{0.5}O_4$). However, this material shows the poorest cyclability of all, similar to that of pure SnO. This suggests that a minimum of network formers is necessary to improve the cycling performance compared with pure SnO.

Fig. 7 shows the potential–discharge capacity profiles for $SnB_{0.5}P_{0.5}O_3$ prepared from different phosphorus supplying starting materials. There are only a few minor differences among the several materials. There is a slightly bigger capacity in the initial reduction step for the material prepared from $Sn_2P_2O_7$. This difference in capacity depends on the length of the described first plateau around 800 mV. The choice of starting material affects only the irreversible capacity during the initial reduction. We could observe no clear differences for subsequent steps.

The cycling performance of these materials (Fig. 8) reveals the same behaviour as discussed. The best cycling performance is provided by the material prepared from P_2O_5. The use of $Sn_2P_2O_7$ as a starting material leads to a very stable reversible capacity around 90 mAh/g.

4. Conclusions

We investigated the suitability and the behaviour of tin-based composite oxides by using electrochemical techniques. For every tin-based oxide irreversible processes occur during the first reduction period, which consume a large amount of lithium. In the case of $SnB_{0.5}P_{0.5}O_3$ a larger amount of lithium is consumed than the theoretical amount needed for the formation of metallic tin and lithium–tin alloys. The use of amorphous tin composite oxides improves the cyclability compared with pure SnO or SnO_2. The specific capacity of the composite oxides depends on their composition. The use of lighter network formers such as boron improves the capacity because of the lowering of the molar mass. The behaviour of tin-based composite oxides is almost independent of the phosphorus supplying starting material.

Compared with the new anode materials announced by Fujifilm the cyclability of our investigated materials is very poor. The mechanism of lithium storage and subsequent anode performance depend on other factors than these investigated here.

Acknowledgements

The authors would like to express their gratitude to Dr. I. Yamada for his continuous guidance and encouragement. They also wish to thank the members of their research group for helpful discussions.

References

[1] D. Fauteux, R. Koksbang, J. Appl. Electrochem. 23 (1993) 1.
[2] T. Shodai, S. Okada, S. Tobishima, J. Yamaki, Solid State Ionics 86 (88) (1996) 785.
[3] N. Koshiba, K. Takata, M. Nakanishi, K. Chikayama, Z. Takehara, Denki Kagaku 62 (1994) 940.
[4] S.Y. Huang, L. Kavan, I. Exnar, M. Grätzel, J. Electrochem. Soc. 142 (1995) L142.
[5] Y. Idota, T. Kubota, A. Matsufuji, Y. Maekawa, T. Miyasaka, Science 276 (1997) 1395.

[6] Y. Idota, Y. Mineo, A. Matsufuji, T. Miyasaka, Denki Kagaku 65 (1997) 717.
[7] I.A. Courtney, J.R. Dahn, Progress in Batteries and Battery Materials 16 (1997) 214.
[8] I.A. Courtney, J.R. Dahn, J. Electrochem. Soc. 144 (1997) 2045.
[9] R.A. Huggins, Electrochem. Soc. Proc. 97 (18) (1997) 1.
[10] T. Ohzuku, Z. Takehara, S. Yoshizawa, Denki Kagaku 46 (1978) 407.
[11] S. Machill, T. Shodai, Y. Sakurai, J. Yamaki, J. Sol. State Electrochem, submitted.